Relay Control of a Morphing Tensegrity Structure with Distributed Pneumatic Actuation

G Lai, A R Plummer
Centre for Power Transmission and Motion Control
Department of Mechanical Engineering
University of Bath, UK
g.lai@bath.ac.uk

Abstract

It is believed that structures and actuation systems should be tightly integrated together in the future to create lightweight dynamic machines. This requires actuators to be distributed through the structure. A tensegrity structure is a very promising candidate for this future integration due to its potentially excellent stiffness and strength-to-weight ratio, and the inherent advantage of being a multi-element structure into which actuators can be embedded. In this paper, an antagonistic multi-axis control of a tensegrity structure is achieved, using a dead band controller. The controller is studied by the describing function technique, and a condition to guarantee stability is derived. The stability condition is illustrated with simulation and experimental results, and is used as a general rule to achieve stable control of the structure.

1. Introduction

Future structures should be tightly integrated with the actuation system, whether for aircraft control, robotic manipulation or other multi-axis applications. This means that actuators will be distributed through the load-bearing structure to allow the structure to morph smartly. These smart structures will provide better static and dynamic performance, redundancy and more adaptability than current designs. With the advent of 'smart' materials, e.g. elastic memory composite, these smart structures are attracting considerable research interest. This is because these materials are deformable as well as load-bearing [1].

A tensegrity structure is deemed to be a very promising candidate for this future integration due to its unique properties. Under natural selection, many living creatures have evolved biomechanical tensegrity structures as it is an optimum solution, e.g. human bones held by muscles and tendons [2]. Tensegrity was first investigated by Emmerich, Fuller and Snelson in 1950s, and was named by Fuller [3]. He created the word tensegrity through the truncation of the phrase "tensional integrity" [4]. The tensegrity is a structure with multiple elements. Some of them are rigid members (struts) and are always in compression. And the rest are flexible members (cables) and are in tension at all times. As its name suggests, the whole structure is required for 'integrity'. In other words, it can only be stabilised by tensile member forces acting on compressive members. All the elements are axially loaded, which means there is no bending moment in any member or torque at any joint. By using knowledge of parallel kinematics, a tensegrity structure can be designed to achieve good stiffness-to-mass ratio without sacrificing the number of degrees of freedom.

Researchers have developed analytical [5-7] and numerical [8-10] methods for the form-finding of tensegrity structures. Analytical methods have been used for tensegrities with relatively simple configuration and tensegrities that have high level of symmetry. For more complicated tensegrities, numerical methods have been used. These methods find the pre-stress level and its corresponding geometric configuration for a given number of members and their interconnections. However, these results are limited as just being stable is not adequate from an engineering point of view. As mentioned in [11], more engineering issues need to be considered. For instance, the nodes where members meet have finite size and thus members cannot meet at the same point in reality.

Tensegrity has numerous applications. Kurilpa Bridge is a multiple-mast, cable-stay structure based on tensegrity principles. In the engineering, tensegrity has been explored most by space applications [12-14] because of the mass efficiency and the capability of being easily stowed and deployed [15].

Actuated tensegrity structures might be useful for aircraft wing morphing. An improvement in aircraft efficiency can be realised if the aircraft can precisely adapt its aerodynamic shape to the ideal form for different flight conditions. Although existing civil aircraft have adopted active shape-changing devices in several components, e.g. leading-edge slats, these devices are only effective for a limited part of the flight regime. The reason is that these control surfaces are connected by hinges which make surfaces discontinuous and can cause the loss of lift or even regional stall [16]. To reduce the surface discontinuity and sharp edges of an aircraft, a possible solution is to replace part of the conventional wing structures with actuated tensegrity structures to perform distributed actuation, which allows subtle changes in curvature. Research [17-19] shows that distributed actuation can provide both redundancy and enhanced aerodynamic efficiency.

Another application example is human-friendly robots. Future robots must interact safely with humans. Conventional industrial arms are too rigid and heavy [20, 21]. An actuated tensegrity structure is an ideal option. Although never pursued, using tensegrity for human-friendly robots was first proposed in 2003 at the University of California [22].

In the authors' previous research [11, 23], a unit cell has been built based on a proposed tensegrity structure.

The unit cell, as shown in Fig. 1, is actuated by pneumatic artificial muscles (PAMs) manufactured by FESTO. The PAM has many advantages over conventional cylinder-type pneumatic actuators, e.g. frictionless and high force to weight ratio [24]. The proposed controller successfully achieves the fundamental control of the position and force of the unit cell. And the presented model replicates the motion and force dynamics of the unit cell reasonably well.

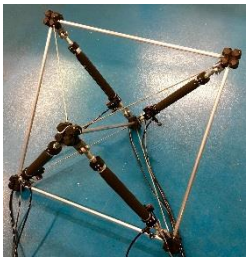

Fig. 1: *Tensegrity unit cell that has been built in University of Bath.*

In this paper, a dead band controller has been used in experiments and simulations. And its stability is analysed. The experimental setup is presented in Section 2. The control of 4 PAMs is described in Section 3. The stability analysis is discussed in Section 4. Experimental results are shown in Section 5, and the conclusions are drawn in Section 6.

2. Experimental actuated tensegrity system

The arrangement of the experimental system is illustrated in Fig. 2. The structure contains two unit cells with a total of 23 members. Among them, nine are struts which are made from aluminium alloy tube. The rest are tensile members, of which ten are stainless steel wires with swage studs at both ends and the remaining four are PAMs embedded in the bottom unit cell. An xPC system is adopted to implement the real-time control and data acquisition for the experimental test. The xPC system has a host PC and a target PC. It allows a controller to be developed as a Simulink model and the model parameters to be tuned on the host PC while running the model in real-time on the target PC. The system provides real-time monitoring of the experimental signals which includes the pressure within the PAM, the displacement of the PAM, and both the position and force demands and their corresponding feedbacks. The force is estimated from the pressure and displacement of the PAM by using a lookup table.

During the actuation, the four PAMs are divided into three different combinations to achieve motions named bend, shear and twist. More details for these three motions are described in [23]. The top unit cell is currently unactuated. The PAM used in this research is type DMSP-20-290N manufactured by FESTO, controlled by two solenoid valves. It has an internal diameter of 20 mm and a nominal length of 290 mm when unpressurised. It has a maximum permissible contraction of 25% of the nominal length and an operational pressure between 0 and 6 bar gauge pressure. When pressurised, the tube of the PAM expands in its circumferential direction, which generates a pulling force and a contraction movement in the longitudinal direction. More information about the experiment, e.g. dimensions of the structure and schematic diagram for the connection of one PAM, can also be found in [23].

3. Antagonistic multi-axis control of the structure

A dead band controller is adopted for both the position and force control. The controller continuously switches the valves on and off until both the demand position and the force are achieved to within a prescribed tolerance where no action occurs, i.e. the output is 0. The control strategy is as shown in Fig. 3.

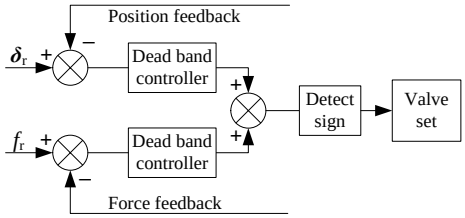

Fig. 3: *Control strategy for the control of the structure.*

There are 3 position loops and a force loop for the control system. For the position loops, the position demands are defined as the deviation of the structure in the three degrees-of-freedom (bend, shear and twist) from the neutral position where all the actuators are of the same length and pre-stress level. Therefore, the position demand, $\boldsymbol{\delta}_r$, is a column vector containing 3 elements. And each element simply represents an actuator length difference for that specific motion. When the structure displaces away from its neutral position, the structure is no longer symmetrical. As a result, the actuator forces will no longer be the same for an appropriately pre-loaded structure. So an average force of the four PAMs is used as the force demand, f_r, in the force loop.

For either loop, if the error is above the dead band, the controller output will be 1. If the error is below the

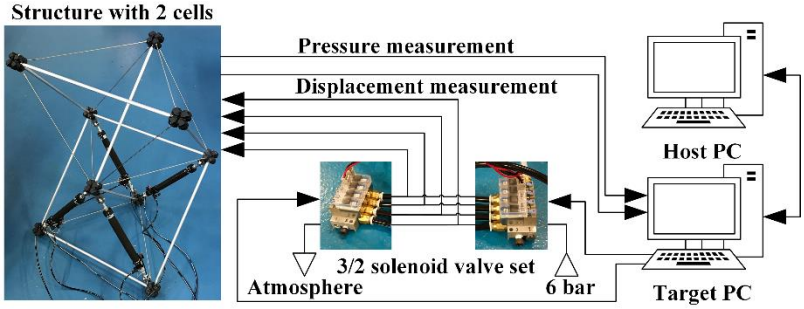

Fig. 2: *Experimental setup for the testing of the structure.*

dead band, the output will be −1. Otherwise, the output will be 0. Each PAM is then controlled according to the combined value of the outputs from the four loops. A positive value will open the high pressure valve. And a negative value will open the low pressure valve. Otherwise, both valves will be closed. The control strategy is essentially based on the multi-axis control scheme proposed in [11].

4. Stability analysis of dead band control system

4.1. Introduction to relay control

The dead band controller is a relay control. As mentioned in the previous section, the controller will continuously switch the valves on and off until the actuating signal lies between the dead band limits where no action occurs, i.e. the output is 0. There is the same level of tolerance for both the positive and negative limits. Other relay controls include bang-bang control and hysteresis control [25]. If the dead band reduces to zero, the controller becomes a bang-bang controller. And the controller turns into a hysteresis controller, also with three operating modes, if the levels of tolerance are inconsistent [25].

The three controllers can all be used to control the structure. However, the bang-bang controller is very energy inefficient as it continually switches. The hysteresis controller requires greater understanding of the dynamics of the system to optimise the tolerance setting. Hence, the dead band controller is chosen.

4.2. Modelling a simplified system

A simple model, analogous to the actuated tensegrity structure, is used to analyse the stability of the dead band controller. A diagram of the system is shown in Fig. 4. A damper and a spring are placed in parallel with a mass attached at one end and a movable base at the other end. The dead band controller can control the base to move left or right at a constant speed to reach different position demands for *y*. The input speed is equivalent to the PAM motion when a valve opens, the spring and damping represents the damped stiffness of the PAMs, and the mass represents the inertia driven by the PAMs.

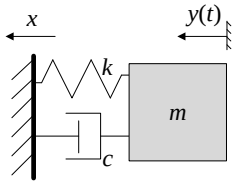

Fig. 4: *Free body diagram of the simplified system.*

The general arrangement of the control system is illustrated in block diagram form in Fig. 5.

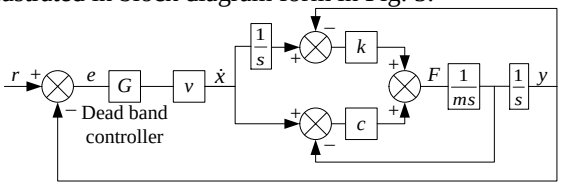

Fig. 5: *Block diagram of the control system.*

In this diagram, *r* is the position demand, *y* is the position feedback and *e* is the error between the two. The output of the dead band controller is:

$$G = \begin{cases} 1 & \text{if } e > B \\ 0 & \text{if } -B \le e \le B \\ -1 & \text{if } e < -B \end{cases} \quad (1)$$

where *B* is the level of tolerance. Thus, the velocity of the movable base is:

$$\dot{x} = Gv \quad (2)$$

where *v* is the speed scaling factor. The spring stiffness and the damping coefficient are represented by *k* and *c* respectively.

4.3. System behaviour with dead band controller

The dead band controller is examined by using the model in Fig. 4. The spring stiffness *k* and the damping coefficient *c* are kept at 500 N/m and 50 Ns/m respectively, and speed constant *v* is 0.014 m/s. Phase plane trajectories are plotted in Figs. 6 to 8 to investigate the system behaviour at different tolerances *B* and masses *m*. The position demand is a step signal of 10 mm. The exploration is carried out in the following sequence. Initially, the tolerance and the mass are set to 1 mm and 6 kg respectively. Secondly, the mass is doubled to 12 kg to see its effect while maintaining the tolerance. Then, based upon the second setting, the tolerance is increased to 1.2 mm.

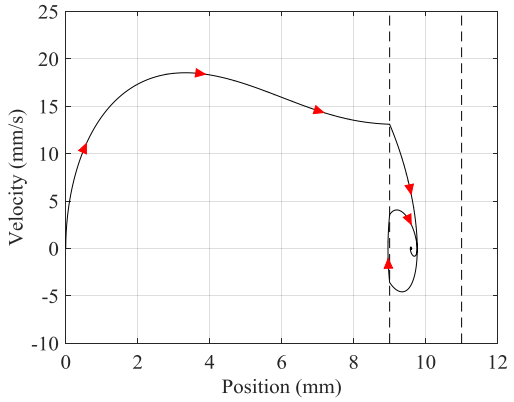

Fig. 6: *Phase plane trajectory with B = 1 mm and m = 6 kg.*

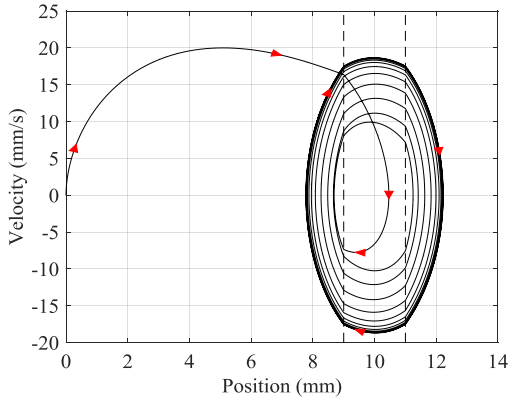

Fig. 7: *Phase plane trajectory with B = 1 mm and m = 12 kg.*

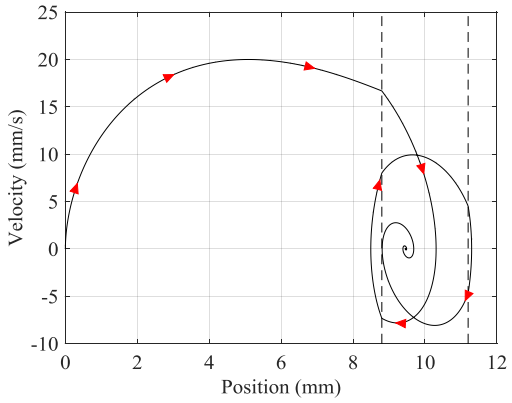

Fig. 8: *Phase plane trajectory with B = 1.2 mm and m = 12 kg.*

In all the trajectory plots, solid arrow heads are used to indicate the direction of the trajectory. Two dash lines are drawn to represent the two dead band limits in each plot. As depicted in Fig. 6, the system is initially stable with the trajectory ending at zero velocity and lying between the dead band limits. When the mass is doubled, Fig. 7, the system becomes unstable. The unstable system oscillates back and forth and spirals into a steady limit cycle. It is observed that the system is stable again, Fig. 8, when the tolerance is increased to 1.2 mm. So the simulation results indicate that increasing the mass can create instability. And an unstable system can be stabilised by increasing the tolerance.

4.4. Describing function of the dead band controller

To analyse the control system, the describing function technique is used [25]. The technique approximates the non-linear part (dead band controller) of the control system by considering the fundamental component of a Fourier series. The describing function is defined as:

$$G_N(M) = \frac{a_1}{M} \tag{3}$$

where a_1 is the fundamental component in the output and M is the amplitude of the excitation waveform.

To simplify the Fourier transform, the excitation and the non-linear output are assumed to be even. So sine terms in the Fourier series can be eliminated. As the integrand has a quarter wave symmetry, the integration range is reduced to one quarter of the period. And the fundamental component is calculated by quadrupling the result.

$$a_1 = 4 \cdot \frac{2}{T}\left[\int_0^{t_2} G\cos(\omega t)dt + \int_{t_2}^{T/4} G\cos(\omega t)dt\right]$$
$$a_1 = \frac{4}{\pi}\sin(\omega t_2) \tag{4}$$

where T is the period, t_2 is the transition time from $G = 1$ to 0, ω is the frequency and t is the time variable.

At the transition time t_2, the value of the excitation waveform equals to the tolerance B which gives:

$$B = M\cos(\omega t_2) \tag{5}$$

By combining Eqs. 3 to 5, the describing function of the dead band controller is derived.

$$G_N(M) = \frac{4}{\pi M}\sqrt{1-\left(\frac{B}{M}\right)^2} \tag{6}$$

with its maximum value,

$$G_N(M)_{\max} = \frac{2}{\pi B} \tag{7}$$

The stability of the non-linear control system can be examined on a Nyquist plot of the product of the describing function and the linear part of the open loop transfer function. However, as the describing function is a function of amplitude and the linear part is a function of frequency, it is more convenient to conduct the examination by plotting the frequency response of the linear part and the negative reciprocal of the describing function. There is a chance of oscillation if they intersect [25]. The linear part of the open loop transfer function of the control system is:

$$D(j\omega) = \frac{k + j\omega c}{j\omega(k - m\omega^2 + j\omega c)} \tag{8}$$

Figure 9 is an example of the examination when the control system is unstable (B = 1 mm and m = 12 kg). It is clear to see that the two plots intersect.

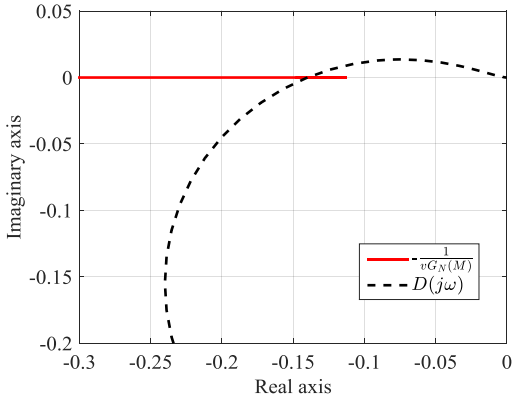

Fig. 9: *Nyquist diagram with B = 1 mm and m = 12 kg.*

4.5. Criterion for guaranteed stability

Therefore, for guaranteed stability of the control system, there should be no intersection. This requires:

$$D(j\omega_{lc}) > -\frac{1}{vG_N(M)_{\max}} \tag{9}$$

where ω_{lc} is the frequency at which the phase of $D(j\omega)$ is −180°.

Equation 8 can be decomposed into the product of an integrator and an expression $A(j\omega)$ which is:

$$A(j\omega) = \frac{k + j\omega c}{(k - m\omega^2) + j\omega c} \tag{10}$$

The frequency at which $\angle A(j\omega) = -90°$ can be found from the right-angle triangle formed by numerator and denominator complex numbers, giving ω_{lc} as:

$$\omega_{lc} = \sqrt{\frac{k^2}{mk - c^2}} \tag{11}$$

By using Eqs. 7 to 9 and 11, an analytical solution for a guaranteed stable response is derived. It requires:

$$\frac{mk - c^2}{ck} < \frac{\pi B}{2v} \tag{12}$$

This analytical solution is consistent with the simulation results (Figs. 6 to 8), indicating that increasing the mass can make the system unstable and increasing the tolerance helps to stabilise the system. The control system is also more likely to be stable with a higher damping coefficient.

5. Experimental results

Experimental results are just presented for the twist motion. Similar behaviours have been observed for the other two motions. The position demand is a square wave of 10 mm amplitude and B = 0.2 mm. It is observed that oscillations occur intermittently as shown in Fig. 10.

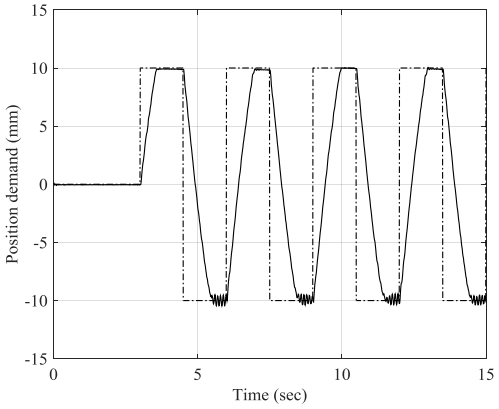

Fig. 10: *Position demand and feedback with a square wave of 10 mm and B = 0.2 mm in the twist motion.*

The oscillations only occur in one direction of the twist motion. This is probably due to the asymmetry of the mass distribution in the tensegrity structure. From the analytical solution, increasing the tolerance should stabilise the system. Figure 11 presents the results when the tolerance is increased to 0.3 mm. It can be seen that there is no oscillation any more.

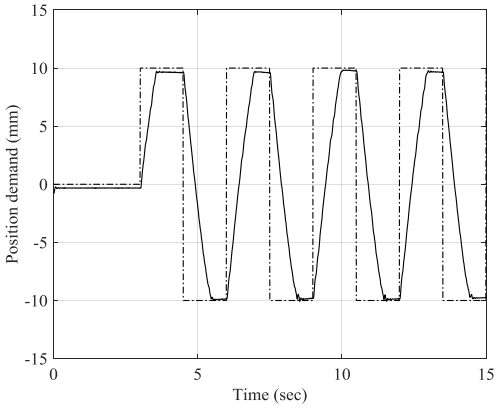

Fig. 11: *Position demand and feedback with a square wave of 10 mm and B = 0.3 mm in the twist motion.*

6. Conclusions

A dead band controller is studied by using the describing function technique. The condition for guaranteed stability is derived and conforms to the simulation results. Combined with the multi-axis control scheme, the proposed dead band controller can actuate the tensegrity structure to achieve motion in three degrees of freedom. In the experimental results presented, limit cycles are observed with a tight dead band tolerance. Learning from the analytical stability condition, the tolerance is increased from 0.2 mm to 0.3 mm, and the system is stabilised. By more detailed analysis of the structure, it should be possible to develop the dead band controller to be adaptive and achieve a robust control without oscillation automatically.

References

[1] Thill C, Etches J, Bond I, Potter K and Weaver P 2008 Morphing skins *Aeronaut. J.* **112**(1129) 117-139

[2] Ingber D E 1997 Tensegrity: The architectural basis of cellular mechanotransduction *Annu. Rev. Physiol.* **59** 575-599

[3] Moored K W and Bart-Smith H 2007 The analysis of tensegrity structures for the design of a morphing wing *J. Appl. Mech.-Trans. ASME* **74**(4) 668-676

[4] Fuller R B 1962 Tensile-Integrity Structures U.S. Patent: 3 063 521

[5] Zhang J Y, Guest S D and Ohsaki M 2009 Symmetric prismatic tensegrity structures. Part II: Symmetry-adapted formulations *International Journal of Solids and Structures* **46**(1) 15-30

[6] Zhang J Y, Guest S D, Connelly R and Ohsaki M 2010 Dihedral 'star' tensegrity structures *International Journal of Solids and Structures* **47**(1) 1-9

[7] Koohestani K and Guest S D 2013 A new approach to the analytical and numerical form-finding of tensegrity structures *International Journal of Solids and Structures* **50**(19) 2995-3007

[8] Koohestani K 2013 A computational framework for the form-finding and design of tensegrity structures *Mech. Res. Commun.* **54** 41-49

[9] Tran H C and Lee J 2013 Form-finding of tensegrity structures using double singular value decomposition *Eng. Comput.* **29**(1) 71-86

[10] Zhang L Y, Li Y, Cao Y P and Feng X Q 2014 Stiffness matrix based form-finding method of tensegrity structures *Eng. Struct.* **58** 36-48

[11] Plummer A and Lai G 2015 *New concepts for parallel kinematic mechanisms using fluid actuation* in *7th International conference on Fluid Power and Mechatronics*. Harbin

[12] Benaroya H 1993 Tensile-Integrity Structures for the Moon *Applied Mechanics Reviews* **46**(6) 326

[13] Tibert A G and Pellegrino S 2002 Deployable tensegrity reflectors for small satellites *J. Spacecr. Rockets* **39**(5) 701-709

[14] Caluwaerts K, Despraz J, Iscen A, Sabelhaus A P, Bruce J, Schrauwen B and SunSpiral V 2014 Design and control of compliant tensegrity robots through simulation and hardware validation *J. R. Soc. Interface* **11**(98) 13

[15] Toklu Y C, Temur R, Bekdas G and Uzun F 2013 Space Applications of Tensegric Structures *Proceedings of 6th International Conference on Recent Advances in Space Technologies* (*Istanbul*) (New York: IEEE) p 29-32

[16] Barbarino S, Bilgen O, Ajaj R M, Friswell M I and Inman D J 2011 A Review of Morphing Aircraft *J. Intell. Mater. Syst. Struct.* **22**(9) 823-877

[17] Gern F H, Inman D J and Kapania R K 2005 Computation of actuation power requirements for smart wings with morphing airfoils *Aiaa J.* **43**(12) 2481-2486

[18] Allen B Designing the 21st Century Aerospace Vehicle - Opening the Door to a New Era in Flight 22 Apr 2008 [cited 2016 26 Jan]; Available from: http://www.nasa.gov/centers/langley/news/factsheets/21stcentury.html

[19] Ramrakhyani D S, Lesieutre G A, Frecker M I and Bharti S 2005 Aircraft Structural Morphing using Tendon-Actuated Compliant Cellular Trusses *Journal of Aircraft* **42**(6) 1614-1620

[20] Salisbury K, Townsend W, Ebrman B and DiPietro D 1988 Preliminary design of a whole-arm manipulation system (WAMS) *Robotics and Automation, 1988. Proceedings., 1988 IEEE International Conference on*: p 254-260 vol.1

[21] Bicchi A and Tonietti G 2004 Fast and "soft-arm" tactics *IEEE Robot. Autom. Mag.* **11**(2) 22-33

[22] Aldrich J B, Skelton R E, Kreutz-Delgado K, Aac and Aac 2003 *Control synthesis for a class of light and agile robotic tensegrity structures* in *Proceedings of the 2003 American Control Conference, Vols 1-6.* Ieee: New York. p 5245-5251

[23] Lai G, Plummer A R, Cleaver D J and Zhou H 2016 Parallel kinematic mechanisms for distributed actuation of future structures *Journal of Physics: Conference Series* **744**(1) 012169

[24] Tondu B 2012 Modelling of the McKibben artificial muscle: A review *J. Intell. Mater. Syst. Struct.* **23**(3) 225-253

[25] Dougherty T 1995 *Systems & Control: An Introduction to Linear, Sampled & Non-linear Systems* (Singapore: World Scientific)